

Analysis of the Spin Exchange Interactions in the Three Phases of Vanadium Pyrophosphate, $(\text{VO})_2\text{P}_2\text{O}_7$, in Terms of Spin–Orbital Interaction Energy

H.-J. Koo and M.-H. Whangbo*

Department of Chemistry, North Carolina State University, Raleigh, North Carolina 27695-8204

Received January 11, 2000

The spin exchange interactions in the ambient-pressure orthorhombic (APO), high-pressure orthorhombic (HPO), and ambient-pressure monoclinic (APM) phases of the vanadium pyrophosphate, $(\text{VO})_2\text{P}_2\text{O}_7$, were analyzed by calculating the spin–orbital interaction energies $\Delta e - \Delta e^0$ of their spin dimers. The anisotropy of the spin exchange interactions in the HPO phase is well explained by the $\Delta e - \Delta e^0$ values. For the APO phase, the reported crystal structure does not provide accurate enough $\Delta e - \Delta e^0$ values to conclude unambiguously which of the V1–V2 and V3–V4 chains has a larger spin gap and which of the bridged and edge-sharing spin dimers has a stronger spin exchange interaction in the V1–V2 and V3–V4 chains. The APM phase is predicted to exhibit essentially two spin gaps, with a large spin gap for the V8–V5–V7–V6 chain and a very small one for the V4–V2–V3–V1 chain.

Introduction

An efficient catalyst for oxidizing *n*-butane to maleic anhydride is vanadium pyrophosphate, $(\text{VO})_2\text{P}_2\text{O}_7$,¹ which is made up of V_2O_8 dimers and pyrophosphates P_2O_7 . A V_2O_8 dimer is obtained from two VO_5 square pyramids by sharing an O–O edge of their basal planes, and a P_2O_7 unit from two PO_4 tetrahedra by sharing an oxygen corner. An important structural feature of $(\text{VO})_2\text{P}_2\text{O}_7$ is the chain of V_2O_8 dimers (hereafter referred to as the dimer chain) in which adjacent V_2O_8 dimers are linked by two PO_4 tetrahedra via the O–P–O bridges. Each vanadium site of $(\text{VO})_2\text{P}_2\text{O}_7$ has a V^{4+} (d^1) cation, and this gives rise to the magnetic properties of $(\text{VO})_2\text{P}_2\text{O}_7$. Since the study of Johnston et al.,² the magnetic properties of $(\text{VO})_2\text{P}_2\text{O}_7$ have received much attention. Their work showed that the ambient-pressure orthorhombic (APO) phase of $(\text{VO})_2\text{P}_2\text{O}_7$ has a singlet ground state and that its magnetic susceptibility is well described by the spin- $1/2$ alternating antiferromagnetic (AFM) chain model although its V^{4+} sublattice is suggestive of spin ladders (assuming that the superexchange interaction via the PO_4 tetrahedra is weak). The spin ladder model describes the magnetic susceptibility of the APO phase well and predicts a spin gap,^{3,4} as does the alternating AFM chain model. However, the later studies proved conclusively that the alternating AFM chain model is correct for the APO phase,^{5,6} and the structural feature leading to this behavior is the dimer chain.^{5–7} The APO phase has two spin gaps⁶ thereby suggesting the presence of two different alternating spin- $1/2$ AFM

Table 1. Spin Gap (K), Spin Exchange Parameters (K), and Nearest-Neighbor V–V Distances (Å) Associated with the Dimer Chains of the APO, HPO, and APM Phases of $(\text{VO})_2\text{P}_2\text{O}_7$

phase	chain type	spin gap	$ J_1/k_B $	$ J_2/k_B $	V–V (OPO) ^d	V–V (O) ^e
HPO ^a		27	137	123	5.23	3.21
APO ^b	V1–V2	68	136	92	5.13	3.26
	V3–V4	35	124	103	5.18	3.18
APM ^c	V4–V2–V3–V1	<i>f</i>	<i>f</i>	<i>f</i>	~5.14	~3.23
	V8–V5–V7–V6	<i>f</i>	<i>f</i>	<i>f</i>	~5.16	~3.21

^a The spin gap and spin exchange parameters were taken from the magnetic susceptibility study of Azuma et al.,⁸ and the V–V distances from the crystal structure study of Azuma et al.⁸ ^b The spin exchange parameters were taken from the inelastic neutron scattering study of Garrett et al.,⁵ the spin gaps from the NMR study of Kikuchi et al.,⁵ and the V–V distances from the crystal structure study of Hiroi et al.⁷ ^c The V–V distances were taken from the crystal structure study of Nguyen et al.⁹ ^d For the intrachain spin dimer. ^e For the edge-sharing spin dimer. ^f Unknown.

chains. This suggestion has been confirmed by the recent crystal structure study.⁷ The high-pressure orthorhombic (HPO) phase of $(\text{VO})_2\text{P}_2\text{O}_7$ consists of identical spin- $1/2$ alternating AFM chains and consequently has a single spin gap.⁸ The magnetic properties of the ambient-pressure monoclinic (APM) phase⁹ of $(\text{VO})_2\text{P}_2\text{O}_7$ have not been reported. The spin gaps, the spin exchange parameters, and the nearest-neighbor V–V distances associated with the dimer chains of the APO and HPO phases are summarized in Table 1.

So far the anisotropy of the spin exchange interactions of $(\text{VO})_2\text{P}_2\text{O}_7$ has not been examined from the viewpoint of the electronic structures of their spin dimers (i.e., structural units containing two adjacent spins). Thus, a number of important questions remain unanswered. It is known that the O–P–O bridges of oxovanadium phosphates provide spin exchange

- (1) Contractor, R. M.; Bergna, H. E.; Horowitz, H. S.; Blackstone, C. M.; Chowdhry, U.; Sleight, A. W. *Catalysis* **1988**, *198*, 645.
- (2) Johnston, D. C.; Johnson, J. W.; Goshorn, D. P.; Jacobson, A. J. *Phys. Rev. B* **1987**, *35*, 219.
- (3) Barnes, T.; Riera, J. *Phys. Rev. B* **1994**, *50*, 6817.
- (4) Eccleston, R. S.; Barnes, T.; Brody, J.; Johnson, J. W. *Phys. Rev. Lett.* **1994**, *73*, 2626.
- (5) Garret, A. W.; Nagler, S. E.; Tennant, D. A.; Sales, B. C.; Barnes, T. *Phys. Rev. Lett.* **1997**, *79*, 745.
- (6) Kikuchi, J.; Motoya, K.; Yamauchi, T.; Ueda, Y. *Phys. Rev. B* **1999**, *60*, 6731.
- (7) Hiroi, Z.; Azuma, M.; Fujishiro, Y.; Saito, T.; Takano, M.; Izumi, F.; Kamiyama, T.; Ikeda, T. *J. Solid State Chem.* **1999**, *146*, 369.

- (8) Azuma, M.; Saito, T.; Fujishiro, Y.; Hiroi, Z.; Takano, M.; Izumi, F.; Kamiyama, T.; Ikeda, T.; Narumi, Y.; Kindo, K. *Phys. Rev. B* **1999**, *60*, 10145.
- (9) Nguyen, P. T.; Hoffman, R. D.; Sleight, A. W. *Mater. Res. Bull.* **1995**, *30*, 1055.

pathways and the way these bridges are arranged determines the magnitude of the spin exchange interaction.^{10,11} However, it is not clear why the spin exchange via the O–P–O bridges is much larger within each dimer chain than between adjacent dimer chains. As already mentioned, the dimer chains of HPO and APO are well described by the spin- $1/2$ alternating AFM chain model.^{5–7} However, it is not known which spin exchange interaction, the one via the PO₄ tetrahedra or that within a V₂O₈ dimer, is larger in magnitude. In the APO phase the larger spin gap was assigned to the dimer chain consisting of the V1 and V2 atoms assuming that in a given type of spin exchange interaction the magnitude of the interaction decreases with increasing V–V distance.^{6,7} It is important to test the validity of this assumption because structural factors other than the V–V distance can influence the interaction between the two magnetic orbitals of a spin dimer. The spin exchange interaction along the *a*-direction (i.e., the ladder direction) is weakly ferromagnetic⁵ rather than AFM, in contrast to the assumption made in the ladder model. The reason for this ferromagnetic interaction has not been explained. In the present work we probe these and related questions by studying the nearest-neighbor spin exchange interactions of the APO, HPO, and APM phases on the basis of the spin dimer analysis.^{12–17} In the following, the spin dimers and spin monomers (i.e., structural units containing a single spin) of these phases were first identified, and then the relative magnitudes of the spin exchange interactions were estimated on the basis of molecular orbital calculations for the spin dimers and monomers.

Crystal Structures and Spin Dimers

To facilitate our discussion, we construct the ideal crystal structures for the APO, HPO, and APM phases of (VO)₂P₂O₇. The APO phase has the “*bc*-plane” layers made up of the dimer chains depicted in Figure 1a, where each square represents a VO₅ square pyramid and a square with solid (dashed) diagonal lines has the apical oxygen atom above (below) the basal plane of the VO₅ square pyramid. In each VO₅ square pyramid the V atom lies above the basal plane such that it makes a shorter V–O bond with the apical oxygen atom than with the basal oxygen atoms. This is a typical geometry found for VO₅ square pyramids containing a V⁴⁺ (d¹) cation.^{18,19} Each triangle represents a P₂O₇ unit (i.e., O₃P–O–PO₃) viewed along the *a*-direction (the P–P axis of P₂O₇ is pointed along the *a*-direction). Each shaded (unshaded) triangle means that the lower (upper) PO₄ tetrahedron of the P₂O₇ unit is corner-shared with three V₂O₈ dimers in a given *bc*-plane layer. Along the *a*-direction, every P₂O₇ unit links two adjacent *bc*-plane layers, so the crystal structure of the APO phase has two *bc*-plane layers per unit cell along the *a*-direction. The crystal structure of the APO phase may also be viewed in terms of the “*ac*-plane” layers of the dimer chains depicted in Figure 1b, where the P₂O₇ units

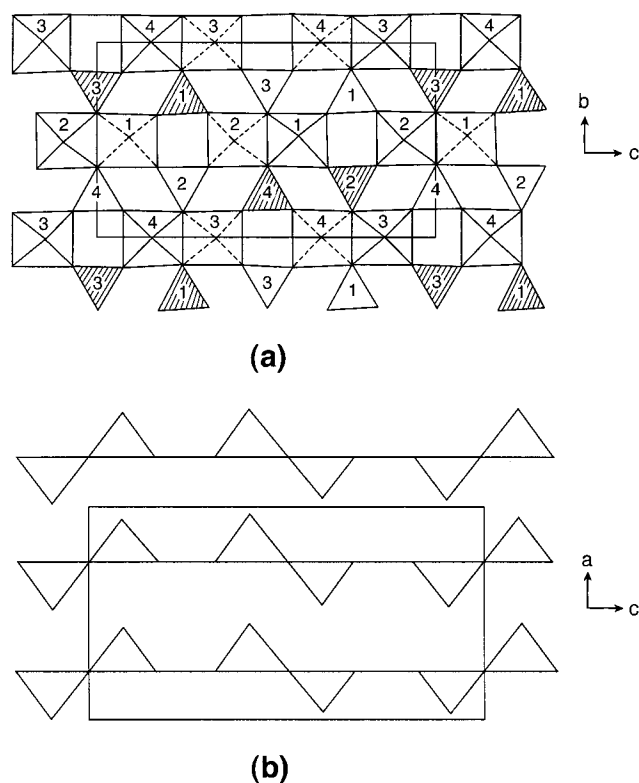


Figure 1. Schematic projection views of the structure of the APO phase: (a) *bc*-plane layer; (b) *ac*-plane layer. In (a) the numbers in the squares and triangles refer to the kinds of the V and P atoms, respectively. In (b) each triangle refers to a VO₅ square pyramid and the pyrophosphate units are not shown for simplicity.

are not shown for simplicity. The crystal structure has two *ac*-plane layers per unit cell along the *b*-direction. The ideal structure of the APM phase is the same as that of the APO phase described above, but this is not the case for the HPO phase. The ideal structure of the HPO phase has the *bc*-plane layers depicted in Figure 2a.

The real structure of the HPO phase⁸ is the same as the ideal structure in that all the V atoms are equivalent, and so are all the P atoms. This is not the case for the real structure of the APO phase,⁷ which has four different V atoms; one dimer chain consists of the V1 and V2 atoms (hereafter referred to as the V1–V2 chain), and the other dimer chain the V3 and V4 atoms (hereafter referred to as the V3–V4 chain). The APO phase has two different P₂O₇ units and four different P atoms; one P₂O₇ unit has the P1–O–P2 linkage, and the other unit the P3–O–P4 linkage. The numbers in the squares and triangles of Figure 1a refer to the kinds of the V and P atoms, respectively, found in the real structure of the APO phase. Adjacent V₂O₈ dimers of each V1–V2 chain are linked by the O–P1–O and O–P2–O bridges, and those of each V3–V4 chain by the O–P3–O and O–P4–O bridges. The APM phase is the same as the APO phase in that each has two different dimer chains. In the APM phase, however, each dimer chain consists of four different V atoms, and a unit cell has four different P₂O₇ units and eight different P atoms. One dimer chain has the V4, V2, V3, and V1 atoms (hereafter referred to as the V4–V2–V3–V1 chain), and the other dimer chain has the V8, V5, V7, and V6 atoms (hereafter referred to as the V8–V5–V7–V6 chain). The P1–O–P4, P2–O–P3, P5–O–P8, and P6–O–P7 linkages are found in the four P₂O₇ units (Figure 2b).⁹

According to the crystal structures described above, the spin monomers of the APO, HPO, and APM phases are represented

(10) Amorós, P.; Beltrán, A.; Beltrán, D. *J. Alloys Comp.* **1992**, *188*, 123.

(11) Roca, M.; Amorós, P.; Cano, J.; Marcos, M. D.; Alamo, J.; Beltrán-Porter, A.; Beltrán-Porter, D. *Inorg. Chem.* **1998**, *37*, 3167.

(12) Lee, K. S.; Koo, H.-J.; Whangbo, M.-H. *Inorg. Chem.* **1999**, *38*, 2199.

(13) Koo, H.-J.; Whangbo, M.-H. *Solid State Commun.* **1999**, *111*, 353.

(14) Whangbo, M.-H.; Koo, H.-J.; Lee, K.-S. *Solid State Commun.* **2000**, *114*, 27.

(15) Koo, H.-J.; Whangbo, M.-H. *J. Solid State Chem.* **2000**, *151*, 96.

(16) Whangbo, M.-H.; Koo, H.-J. *Solid State Commun.*, in press.

(17) Koo, H.-J.; Whangbo, M.-H. *J. Solid State Chem.*, in press.

(18) Wheeler, R. A.; Whangbo, M.-H.; Hughbanks, T.; Hoffmann, R.; Burdett, J. K.; Albright, T. A. *J. Am. Chem. Soc.* **1986**, *108*, 2222.

(19) Whangbo, M.-H. In *Crystal Chemistry and Properties of Materials with Quasi-One Dimensional Structures*; Rouxel, J., Ed.; Reidel: Dordrecht, The Netherlands, 1986; p 27.

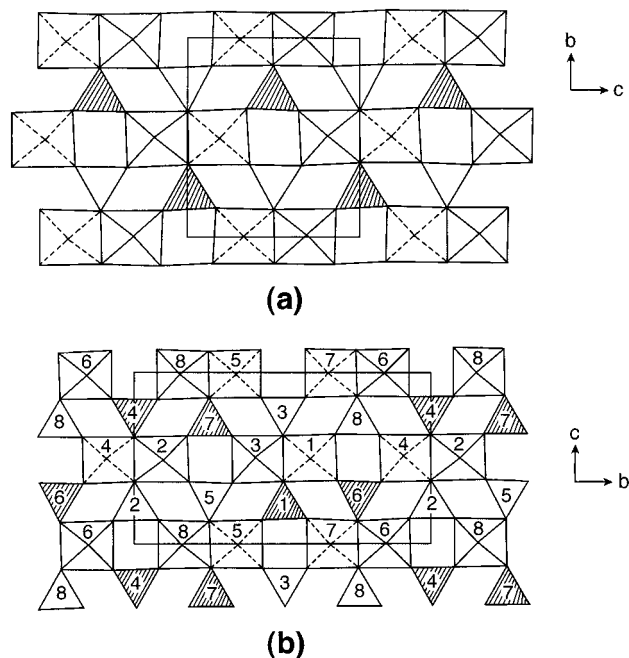


Figure 2. Schematic projection views of the bc -plane layers of the (a) HPO and (b) APM phases. In (b) the numbers in the squares and triangles refer to the kinds of the V and P atoms, respectively.

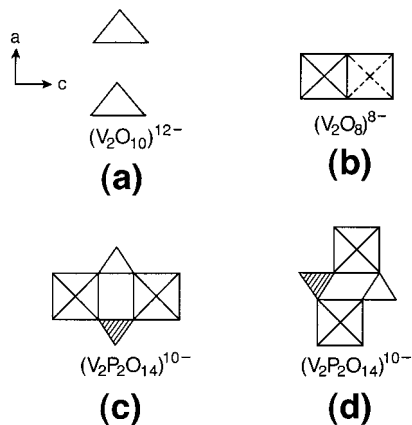


Figure 3. Schematic projection views of (a) a spin dimer $(\text{V}_2\text{O}_{10})^{12-}$ along the a -direction, (b) an edge-sharing spin dimer $(\text{V}_2\text{O}_8)^{8-}$, (c) an intrachain bridged spin dimer $(\text{V}_2\text{P}_2\text{O}_{14})^{10-}$, and (d) an interchain bridged spin dimer $(\text{V}_2\text{P}_2\text{O}_{14})^{10-}$.

by the $(\text{VO}_5)^{6-}$ ions. There are several different kinds of spin dimers to consider. Along the a -direction, a spin dimer consists of two isolated VO_5 square pyramids and has the formula $(\text{V}_2\text{O}_{10})^{12-}$ (Figure 3a). Each dimer chain has two different spin dimers, an edge-sharing spin dimer $(\text{V}_2\text{O}_8)^{8-}$ (Figure 3b) and a bridged spin dimer in which two VO_5 square pyramids are linked by two PO_4 units (e.g., Figure 3c). (To simplify our calculations, each P_2O_7 unit of a bridged spin dimer is replaced with the PO_4 unit directly attached to the VO_5 square pyramids.) Thus the formula of a bridged spin dimer is given by $(\text{V}_2\text{P}_2\text{O}_{14})^{10-}$. Similar spin dimers occur between adjacent dimer chains (e.g., Figure 3d). To assess the role of the O–P–O bridges in a bridged spin dimer $(\text{V}_2\text{P}_2\text{O}_{14})^{10-}$, we also consider the spin dimer $(\text{V}_2\text{O}_{10})^{12-}$ obtained from the bridged spin dimer by removing the O–P–O bridges.

Spin–Orbital Interaction Energy

The nearest-neighbor spin exchange parameter J of a spin dimer is related to the energy difference ΔE between the triplet

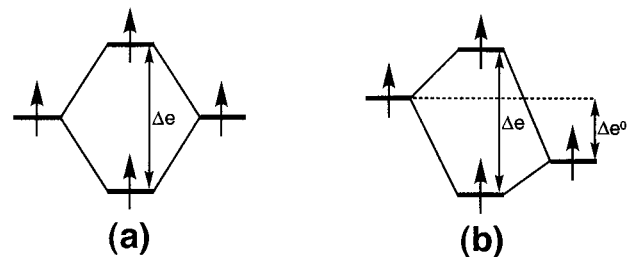


Figure 4. Interaction between spin monomers leading to the two singly filled energy levels of a spin dimer: (a) between equivalent spin monomers; (b) between nonequivalent spin monomers.

and singlet states of the corresponding spin dimer, i.e., $J = \Delta E = {}^1E - {}^3E$.^{20–22} In general, J is written as $J = J_F + J_{AF}$, where the ferromagnetic term J_F favors the triplet state (i.e., $J_F > 0$), while the antiferromagnetic term J_{AF} favors the singlet state (i.e., $J_{AF} < 0$). Qualitative trends in the J parameters of an extended magnetic solid can be discussed in terms of one-electron orbital energies of spin dimers obtained from extended Hückel molecular orbital calculations.^{23,24} For the interaction between two equivalent spins, $|J_{AF}|$ increases with increasing Δe , where Δe is the energy separation between the highest two singly occupied energy levels of a spin dimer (Figure 4a).^{20,21} For the interaction between two nonequivalent spins, $|J_{AF}|$ increases with the net change in orbital energy, $\Delta e - \Delta e^0$ (Figure 4b).^{14,25} For AFM systems, the variation of the $|J|$ parameters can be understood by studying that of the corresponding $\Delta e - \Delta e^0$ values (for the interaction between two equivalent spins, $\Delta e^0 = 0$), as shown for a large number of ternary transition metal oxides and fluorides.^{12–17} The spin exchange interaction of a spin dimer is most likely to be ferromagnetic when the $\Delta e - \Delta e^0$ value is negligible. In the present work this spin-dimer analysis was carried out for the APO, HPO, and APM phases. The parameters of the atomic orbitals used in our calculations were taken from our previous work.^{12,13,26} Double- ζ Slater type orbitals²⁷ were used for the d orbitals of V and for the 2s/2p orbitals of O, because diffuse components of these orbitals provide diffuse tails crucial for intermolecular overlap.^{12–17}

The $\Delta e - \Delta e^0$ values calculated for the various spin dimers of the APO, HPO, and APM phases of $(\text{VO})_2\text{P}_2\text{O}_7$ are summarized in Table 2. For the edge- and bridge-sharing spin dimers, the legends trans and cis indicate that the apical oxygen atoms occur on the opposite sides and on a same side of the basal plane, respectively. To assess the role of the O–P–O linkages of a bridged spin dimer $(\text{V}_2\text{P}_2\text{O}_{14})^{10-}$, the $\Delta e - \Delta e^0$ value was also calculated for the spin dimer $(\text{V}_2\text{O}_{10})^{12-}$ that results from the bridged spin dimer by removing the O–P–O bridges. Such $\Delta e - \Delta e^0$ values are listed in parentheses in Table 2. For each bridged spin dimer of the APO and APM phases, the numbers in brackets refer to the kinds of the V and P atoms associated with the spin dimer.

- (20) Hay, P. J.; Thibault, J. C.; Hoffmann, R. *J. Am. Chem. Soc.* **1975**, *97*, 4884.
 (21) Kahn, O.; Briat, B. *J. Chem. Soc., Faraday Trans. II* **1976**, *72*, 268.
 (22) For calculations of ΔE based on first principles electronic structure methods, see: Moreira, I. d. P. R.; Illas, F.; Calzado, C. J.; Sanz, J. F.; Malrieu, J.-P.; Amor, N. B.; Maynau, D. *Phys. Rev. B* **1999**, *59*, 6593 and references therein.
 (23) Hoffmann, R. *J. Chem. Phys.* **1967**, *39*, 1397.
 (24) Our calculations were carried out by employing the CAESAR program package (Ren, J.; Liang, W.; Whangbo, M.-H. *Crystal and Electronic Structure Analysis Using CAESAR*; 1998. This book can be downloaded free of charge from the web site <http://www.PrimeC.com/>.)
 (25) Kahn, O. *Struct. Bonding* **1987**, *68*, 89.
 (26) Long, V. C.; Musfeldt, J. L.; Wei, X.; Koo, H.-J.; Whangbo, M.-H.; Jegoudez, J.; Revcolevschi, A. *Phys. Rev. B* **1999**, *60*, 15721.
 (27) Clementi, E.; Roetti, C. *At. Data Nucl. Data Tables* **1974**, *14*, 177.

Table 2. $\Delta e - \Delta e^0$ Values (meV) Calculated for the Spin Dimers of $(\text{VO})_2\text{P}_2\text{O}_7^{a,b}$

phase	along a^c	edge-sharing ^c	bridged/intrachain ^d	bridged/interchain ^d
HPO	2	78, trans	87 (117), trans	11 (34), cis
APO	2 [1,1]	65 [1,2], trans	56 (78) [1,2/1,2], cis	13 (36) [1,4/1,3], trans
	1 [2,2]	28 [3,4], trans	39 (48) [3,4/3,4], cis	13 (13) [1,4/2,4], trans
	2 [3,3]			0 (6) [2,3/1,3], cis
	1 [4,4]			0 (0) [2,3/2,4], cis
APM	0 [1,2]	50 [2,4], trans	46 (63) [1,4/6,8], cis	22 (44) [1,7/1,6], cis
	3 [3,4]	47 [1,3], trans	49 (69) [2,3/5,7], cis	16 (38) [2,8/2,5], cis
	0 [5,6]	69 [5,8], trans	82 (106) [5,7/1,3], cis	9 (29) [1,7/3,8], cis
	0 [7,8]	66 [6,7], trans	88 (112) [6,8/2,4], cis	7 (25) [2,8/4,7], cis 2 (11) [4,6/4,8], trans 1 (11) [3,5/3,7], trans 6 (8) [3,5/1,5], trans 5 (5) [4,6/2,6], trans

^a For the bridged spin dimers, the $\Delta e - \Delta e^0$ values calculated without the O–P–O linkages are listed without parentheses, and those calculated with the O–P–O linkages are given in parentheses. ^b For the edge- and bridge-sharing spin dimers, the legends trans and cis indicate that the apical oxygen atoms occur on the opposite sides and on a same side of the basal plane, respectively. ^c The numbers in a bracket for each edge-sharing spin dimer refer to the kinds of the vanadium atoms contained in the spin dimer. For example, [1,2] means that the spin dimer consists of the V1 and V2 atoms. ^d The numbers in a bracket for each bridged spin dimer refer to the kinds of the V and P atoms associated with the spin dimer. For example, [1,4/6,8] means that the spin dimer consists of the V1 and V4 atoms, and the spin dimer has O–P6–O and O–P8–O bridges.

Results and Discussion

A. HPO Phase. The $\Delta e - \Delta e^0$ value is negligible along the a -direction, is small between adjacent dimer chains, and is large within each dimer chain. The bridged and edge-sharing spin dimers in each dimer chain have different $\Delta e - \Delta e^0$ values. These results are consistent with the fact that the magnetic susceptibility of the HPO phase is well described by the spin- $1/2$ alternating AFM chain model.⁸

The spin exchange interaction in the a -direction is expected to be ferromagnetic because the corresponding $\Delta e - \Delta e^0$ value is negligible (as in the case of the APO phase to be discussed below). The $\Delta e - \Delta e^0$ value is much larger for the intrachain than for the interchain bridged spin dimer. The O–P–O bridges enhance the $\Delta e - \Delta e^0$ value for the intrachain and interchain bridged spin dimers. This is consistent with the observation that in oxovanadium phosphates the O–P–O bridges provide spin exchange pathways.^{10,11} However, the enhancement of $\Delta e - \Delta e^0$ by the O–P–O bridges is nearly the same for the intrachain and interchain bridged spin dimers (about 24 meV). Furthermore the $\Delta e - \Delta e^0$ value is larger for the intrachain than for the interchain bridged spin dimer even in the absence of the O–P–O bridges. Thus, the magnitude of the spin exchange interaction in a bridged spin dimer is determined mainly by the way its two VO_5 square pyramids are arranged rather than by the O–P–O bridges.

To explain the above observations, it is necessary to consider the magnetic orbital of a spin monomer $(\text{VO}_5)^{6-}$ (Figure 5a). Given the local Cartesian x - and y -axes along the V–O bonds of the basal plane, the magnetic orbital of a spin monomer is largely given by the xy -orbital of V, which is combined out-of-phase with the p orbital of each basal oxygen atom. Along the a -direction, the two magnetic orbitals of a spin dimer have a δ -type overlap (Figure 5b), so the $\Delta e - \Delta e^0$ value becomes negligible. The two magnetic orbitals in the intrachain and interchain bridged spin dimers have a σ -type overlap through the O···O contacts, as depicted in Figure 5c,d, respectively. The values of the various O···O contact distances defined in Figure 5c,d are listed in Tables 3 and 4, respectively. The σ -type overlap of the intrachain bridged spin dimer is determined mainly by the short O···O contacts a and a' than by the long O···O contacts b and b' (Figure 5c). However, the σ -type overlap of the interchain bridged spin dimer is determined mainly by the “diagonal” O···O contact c than by the short “nondiagonal” O···O contacts d and d' (Figure 5d), because in the O···O

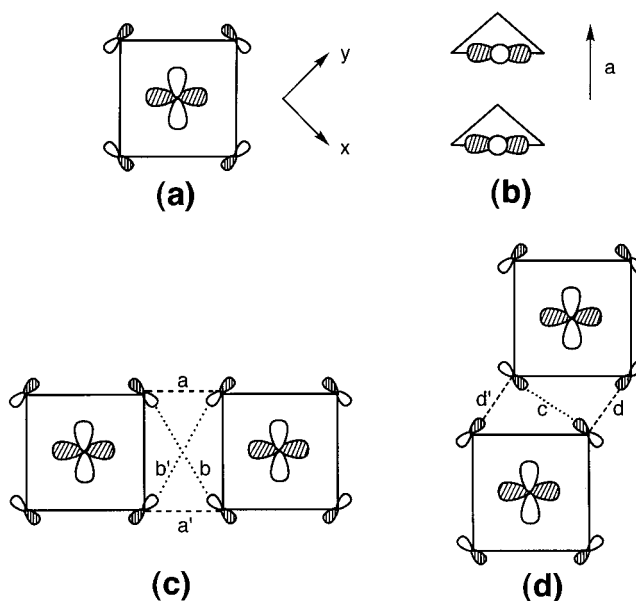


Figure 5. (a) Magnetic orbital of a spin monomer $(\text{VO}_5)^{6-}$, (b) δ -type overlap between the magnetic orbitals in a spin dimer along the a -direction, (c) σ -type overlap between the magnetic orbitals in an intrachain bridged spin dimer, and (d) σ -type overlap between the magnetic orbitals in an interchain bridged spin dimer. In (c) and (d) the diagonal O···O contacts are indicated by dotted lines, and the nondiagonal O···O contacts by dashed lines.

contact c the oxygen orbitals are aligned along the contact direction while in the O···O contact d or d' one oxygen p orbital lies almost in the nodal plane of the other oxygen p orbital. The diagonal O···O contact distance c of the interchain bridged spin dimer is longer than the nondiagonal O···O contacts a and a' of the intrachain bridged spin dimers (Tables 3 and 4). Furthermore, the σ -type overlap occurs mainly through two O···O contacts (i.e., a and a') in the intrachain bridged spin dimer but mainly through one diagonal O···O contact (i.e., c) in the interchain bridged spin dimer. This explains why the $\Delta e - \Delta e^0$ value is larger for the intrachain than for the interchain spin dimer.

In each dimer chain the $\Delta e - \Delta e^0$ value is larger for the bridged than for the edge-sharing spin dimer. It should be noticed that the superexchange via the O–P–O bridges is not the sole cause for this observation because the same is true even when the O–P–O bridges are removed from the bridged spin

Table 3. O···O Distances (Å) of the Intrachain Bridged Spin Dimers in (VO)₂P₂O₇^a

phase	dimer type ^b	<i>a</i>	<i>a'</i>	<i>b</i>	<i>b'</i>
HPO		2.52	2.52	3.59	3.86
APO	[1,2/1,2]	2.56	2.53	3.59	3.68
	[3,4/3,4]	2.46	2.49	3.71	3.73
APM	[1,4/6,8]	2.54	2.52	3.51	3.69
	[2,3/5,7]	2.55	2.53	3.53	3.67
	[5,7/1,3]	2.52	2.54	3.71	3.80
	[6,8/2,4]	2.51	2.52	3.71	3.79

^a The O···O contact distances *a*, *a'*, *b*, and *b'* are defined in Figure 5c. ^b The numbers in a bracket for each bridged spin dimer refer to the kinds of the V and P atoms associated with the spin dimer. For example, [1,4/6,8] means that the spin dimer consists of the V1 and V4 atoms, and the spin dimer has O–P6–O and O–P8–O bridges.

Table 4. O···O Distances (Å) of the Interchain Bridged Spin Dimers in (VO)₂P₂O₇^a

phase	dimer type ^b	<i>c</i>	<i>d</i>	<i>d'</i>
HPO		2.70	2.53	2.49
APO	[1,4/1,3]	2.67	2.53	2.44
	[1,4/2,4]	2.75	2.53	2.53
	[2,3/1,3]	2.72	2.54	2.43
	[2,3/2,4]	2.72	2.53	2.47
APM	[1,7/1,6]	2.67	2.50	2.50
	[2,8/2,5]	2.69	2.51	2.50
	[1,7/3,8]	2.71	2.51	2.51
	[2,8/4,7]	2.72	2.50	2.52
	[4,6/4,8]	2.73	2.47	2.51
	[3,5/3,7]	2.75	2.51	2.53
	[3,5/1,5]	2.75	2.51	2.49
	[4,6/2,6]	2.76	2.53	2.50

^a The O···O contact distances *c*, *d*, and *d'* are defined in Figure 5d. ^b The numbers in a bracket for each bridged spin dimer refer to the kinds of the V and P atoms associated with the spin dimer. For example, [1,4/1,3] means that the spin dimer consists of the V1 and V4 atoms, and the spin dimer has O–P1–O and O–P3–O bridges.

dimer. The analysis of the magnetic susceptibility data by Azuma et al.⁸ showed that the difference between the *J*₁ and *J*₂ values is small (Table 1) and that the spin exchange interaction between dimer chains is negligible. These two findings are quite well reproduced if the $\Delta e - \Delta e^0$ values of the bridged spin dimers calculated without the O–P–O bridges are used for comparison. It is clear that our calculations overestimate the role of the superexchange interaction that takes place through the O–P–O bridges.

B. APO Phase. The reported crystal structure of the APO phase is not so accurate as that of the HPO phase. The fractional coordinates of all the V and O atoms were reported with three-digit accuracy for the APO phase⁷ but with four-digit accuracy for the HPO phase.⁸ Consequently, the $\Delta e - \Delta e^0$ values calculated for the APO phase have a limited validity, as discussed below.

Table 2 shows that the $\Delta e - \Delta e^0$ value along the *a*-direction is negligible, in agreement with the fact that the corresponding spin exchange interaction is weakly ferromagnetic.⁵ The analysis of the inelastic neutron scattering data by Garrett et al.⁵ showed that the spin exchange interaction between dimer chains is negligible. This observation is reproduced by the $\Delta e - \Delta e^0$ values of the bridged spin dimers calculated without the O–P–O bridges, just as in the case of the HPO phase. Thus in the remainder of this section, our discussion will be based on the $\Delta e - \Delta e^0$ values of the bridged spin dimers calculated without the O–P–O bridges.

For the intrachain interactions Table 2 shows that the $\Delta e - \Delta e^0$ value is larger for the bridged spin dimer than for the edge-

sharing spin dimer in the V3–V4 chain, but the opposite is the case for the V1–V2 chain. These $\Delta e - \Delta e^0$ values suggest a greater alternation of spin exchange interaction, and hence a larger spin gap, for the V3–V4 chain than for the V1–V2 chain. This is contrary to the assignment made by Kikuchi et al.⁶ and by Hiroi et al.⁷ assuming that (a) the spin exchange interaction is stronger for the bridged than for the edge-sharing spin dimer and (b) the interaction becomes weaker with increasing the V–V distance for both spin dimers. Our calculations support the assumption a for the V3–V4 chain but not for the V1–V2 chain. Comparison of the nearest-neighbor V–V distances and the $\Delta e - \Delta e^0$ values (Tables 1 and 2) shows that our calculations support the assumption b for the bridged spin dimers but not for the edge-sharing spin dimers. Thus, concerning whether the assumptions a and b are correct, our calculations do not provide a clear-cut answer. Furthermore, the intrachain $\Delta e - \Delta e^0$ values for the V1–V2 and V3–V4 chains are considerably smaller than the corresponding values of the HPO phase, which is certainly inconsistent with the experimental observation that the intrachain spin exchange parameters of the HPO phase are comparable in magnitude with those of the APO phase (Table 1). These difficulties are due in part to the fact that the atom positions of the APO phase are not precise enough for accurate spin–orbital interaction energy calculations. To illustrate this point, we first note that the crystal structure of the APO phase reported by Hiroi et al.⁷ has the largest *B*_{eq} parameter for the O16 atom⁷ and then examine how the position of this atom affects the $\Delta e - \Delta e^0$ values for the edge-sharing and the bridged spin dimers in the V3–V4 chain. The $\Delta e - \Delta e^0$ values are 28 and 39 (48) meV, respectively, when the reported *x*-, *y*-, and *z*-coordinates of the O16 are used as listed in Table 2 but increase to 34 and 49 (60) meV (decrease to 24 and 38 (32) meV), respectively, when the *x*-, *y*- and *z*-coordinates of the O16 are chosen as the smallest (largest) possible values allowed by the given standard deviations. Such a large change in $\Delta e - \Delta e^0$ indicates that electronic structure calculations based on the reported crystal structure of the APO phase have a limited utility. A more accurate crystal structure of the APO phase is needed to determine conclusively which of the V1–V2 and V3–V4 chains has a larger spin gap and also which of the bridged and edge-sharing spin dimers has a stronger spin exchange interaction in the V1–V2 and V3–V4 chains.

C. APM Phase. The crystal structure of the APM phase is more accurate than that of the APO phase but is somewhat less accurate than that of the HPO phase. All the fractional coordinates of the V, P, and O atoms of the APM phase were reported with four-digit accuracy, except for the 10 out of the 56 O atoms in a unit cell, whose fractional *x*-coordinates were reported with three-digit accuracy.⁹ Each dimer chain of the APM phase has two edge-sharing and two bridged spin dimers (Figure 2b). The previous two sections showed that for the bridged spin dimers, the $\Delta e - \Delta e^0$ values calculated without the O–P–O bridges are more reliable than are those with the O–P–O bridges. It is reasonable to assume that this is also the case for the APM phase. Thus in this section, our discussion will be based on the $\Delta e - \Delta e^0$ values of the bridged spin dimers calculated without the O–P–O bridges.

The $\Delta e - \Delta e^0$ values calculated for the APM phase show that the spin exchange interaction is stronger for the bridged spin dimer than for the edge-sharing spin dimer in the V8–V5–V7–V6 chain, but the spin exchange interactions of the two spin dimers are similar in the V4–V2–V3–V1 chain. In each dimer chain the two edge-sharing spin dimers are practically similar, and so are the two bridged spin dimers. Thus each

dimer chain of the APM phase is expected to exhibit one spin gap. However, it should be noted that the $\Delta e - \Delta e^0$ values of the bridged and edge-sharing spin dimers have a large difference in the V8–V5–V7–V6 chain but a very small difference in the V4–V2–V3–V1 chain. As a consequence, it might be difficult to detect a spin gap of the V4–V2–V3–V1 chain. This picture is in contradiction to that of Kikuchi et al.,⁶ who suggested on the basis of the assumptions a and b (see the previous section) that the spin gap should be higher for the V4–V2–V3–V1 chain than for the V8–V5–V7–V6 chain. As in the cases of the APO phase, their assumption b is not quite well satisfied for the APM phase; this assumption is not supported for the bridged spin dimers but for the edge-sharing spin dimers.

Concluding Remarks

For all the APO, HPO, and APM phases, the spin–orbital interaction energy $\Delta e - \Delta e^0$ is negligible along the *a*-direction and is generally larger for the intrachain than for the interchain bridged spin dimer. These results are readily explained by considering the overlap between the magnetic orbitals in a spin dimer, which is determined largely by the O···O contacts. Our calculations show that the O–P–O bridges of a bridged spin dimer enhance the $\Delta e - \Delta e^0$ value. However, comparison of the $\Delta e - \Delta e^0$ values with the experimental spin exchange parameters for the HPO and APO phases shows that our calculations exaggerate the spin exchange interaction occurring through the O–P–O bridges and that for the bridged spin dimers the $\Delta e - \Delta e^0$ values calculated without the O–P–O bridges are more consistent with experiment than are those calculated with the O–P–O bridges.

For the HPO phase, an accurate crystal structure is available, the trends in the $\Delta e - \Delta e^0$ values based on this crystal structure are in good agreement with those in the spin exchange parameters determined experimentally, and the spin exchange interaction within each dimer chain is slightly stronger for the bridged spin dimer than for the edge-sharing spin dimer. For the APO phase, the $\Delta e - \Delta e^0$ values based on the reported crystal structure are not accurate enough to conclude unambiguously which of the V1–V2 and V3–V4 chains has a larger spin gap and which of the bridged and edge-sharing spin dimers has a stronger spin exchange interaction in the V1–V2 and V3–V4 chains. It is desirable to have a more accurate crystal structure of the APO phase. Our study predicts that practically the APM phase will exhibit two spin gaps, with a large spin gap for the V8–V5–V7–V6 chain and a very small one for the V4–V2–V3–V1 chain.

The $\Delta e - \Delta e^0$ values calculated for the APO and APM phases do not quite well support the assumption that the spin exchange interaction in the intrachain bridged or the edge-sharing spin dimer becomes weaker with increasing V–V distance. Whether or not this is due to the inaccuracy of the reported crystal structures remains to be studied further.

Acknowledgment. Work at North Carolina State University was supported by the Office of Basic Energy Sciences, Division of Materials Sciences, U.S. Department of Energy, under Grant DE-FG05-86ER45259.

IC000046T